Applicability of spaceborne lidar measurements to study shallow marine convection over the subtropical North Atlantic Ocean

Manuel Gutleben[1], Silke Groß[1], Martin Wirth[1], Florian Ewald[1], and Andreas Schäfler[1]

[1]Deutsches Zentrum für Luft- und Raumfahrt (DLR), Institut für Physik der Atmosphäre, 82234 Wessling, Germany.

Correspondence to: MANUEL GUTLEBEN (manuel.gutleben@dlr.de)

Abstract. Airborne lidar measurements over the subtropical North Atlantic Ocean were performed to study shallow marine convection. One focus of those measurements was on the evaluation of satellite-based lidar measurements, by means of co-ordinated underflights. Satellite lidar and radar measurements form a good basis to derive cloud size parameters, which are important for the parametrization of shallow marine convection in climate models. In this study we use a large number of satellite underflights performed during these research flights, to directly compare satellite lidar measurements with high resolution airborne lidar measurements. This allows us to test the applicability of satellite lidar instruments for the detection of shallow marine convection. Statistics of shallow marine cloud size parameters, e.g. cloud top height distributions, are in good agreement, however, cloudy/cloud-free segments of less than 330 m extent cannot be resolved by the CALIOP instrument, resulting in an underestimation of small cloud and cloud gap lengths.

1 Introduction

Shallow clouds have a significant impact on the Earth's radiation budget (Bony and Dufresne, 2005) and are one of the dominant contributors to global albedo (Hartmann et al., 1992). As a result, differences in the representation of shallow marine convection in global climate models lead to large differences in climate sensitivity estimates (Bony and Dufresne (2005); Zelinka et al. (2012)). Since those cumulus clouds are often of smaller extent than grid spacings of General Circulation Models, they have to be parametrized. Crucial properties for parametrizations are cloud macrophysical properties, i.e. cloud top height distributions, cloud fractions, cloud lengths and cloud gap lengths. However, due to the remote geographical location of shallow marine convection over the Earth's subtropical oceans, high resolution measurements of cloud size parameters are limited and only possible in the course of shipborne or airborne field campaigns (e.g. Colòn-Robles et al. (2006), Siebert et al. (2013)). Satellite measurements are the major source for retrieving those properties, as they provide long-term measurements with nearly global coverage. In this context, passive as well as active remote sensing techniques with the lidar Cloud-Aerosol Lidar with Orthogonal Polarization (CALIOP; Winker et al. (2007)) on board the Cloud-Aerosol Lidar and Infrared Pathfinder Satellite Observations (CALIPSO; Winker et al. (2010)) satellite are used. Passive instruments suffer from poor horizontal resolution and provide only limited or even no vertical information on the measurements. In contrast, CALIOP has a resolution of 330 m in the horizontal and 30 m in the vertical. However, the majority of shallow marine clouds has an extent of just a few hundred meters (Wood and Field, 2000).

Consequently questions arise, if the resolution of CALIOP is sufficient for detecting shallow marine cumulus clouds and, if CALIOP measurements are suitable to serve as input regarding shallow marine cloud size parametrizations in General Circulation Models.

In December 2013, airborne measurements with the German research aircraft HALO (High Altitude and LOng range; Krautstrunk and Giez (2012)), were performed during the Next-generation Airborne Remote sensing for VALidation studies (NARVAL; Klepp et al. (2014)). HALO is a modified Gulfstream G550 business jet with a maximum range of more than 12000 km and a maximum cruising altitude of more than 15500 m. Thus, HALO enables to perform long measurement legs to remote areas over the subtropical North Atlantic Ocean. During NARVAL, the HALO aircraft was equipped with two core instrument packages, an advanced lidar system and the Halo microwave package (HAMP), a combination of a 36 GHz cloud radar and a set of microwave radiometers (Mech et al., 2014). The aim of the campaign was to study shallow marine trade wind convection and its environment. One main focus of the measurements was set on the undeflights of CALIPSO and CloudSat (Stephens et al., 2002) for the comparison of satellite measurements with airborne measurements.

In this work we focus on lidar measurements to derive cloud macrophysical properties of shallow marine convection, i.e. cloud top height, cloud length and cloud gap length statsitsics.

This article is structured as follows: Section 2 gives an overview of the mission, instrumentation and used method. Section 3 presents the comparison of airborne and space-borne derived cloud size properties, and Section 4 discusses and concludes this work.

2 Method and instrumentation

2.1 NARVAL

The aim of the NARVAL mission in December 2013 was to study shallow marine convection over the subtropical North-Atlantic Ocean in the Carribean dry season. During NARVAL the HALO aircraft was equipped with a set of remote sensing instruments. Besides the two main instrument packages, an advanced lidar system and the combined cloud radar and microwave package (HAMP, Mech et al. (2014)), the payload also included instruments for radiation measurements. Altogether eight measurement flights with almost 70 flight hours were conducted in the period from 10 to 20 December 2013 (Figure 1). Four of these measurement flights were conducted from and to Oberpfaffenhofen (EDMO, Germany) to study the transition from extratropical weather regimes to trade wind regimes (transfer flights). The other four research flights departed from Grantley Adams Airport (TBPB, Barbados) and were dedicated to the investigation of shallow marine convection (local flights). For each of the research flights an underflight of the CALIPSO and CloudSat satellites was planned. However, on 19 December the underflight had to be cancelled due to bad weather conditions. Table 1 gives an overview of measurement dates and times, including the times of the satellite underflights.

As our main focus in this study is on macrophysical properties of shallow marine trade wind convection, we only use measurements in latitudes from 10° N to 20° N and in heights up to 4 km (Stevens, 2005). To further exclude influences from landmasses we restrict our analysis to an area between 35° W and 60° W.

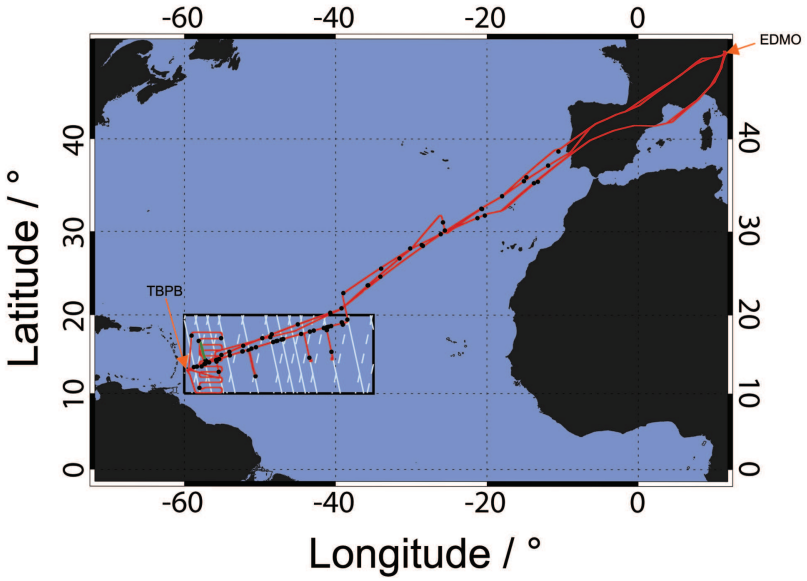

Figure 1. Flight-tracks of CALIPSO and HALO during NARVAL. White lines represent CALIPSO flightpaths of interest ranging from $60°W$ to $35°W$ and $10°$ to $20°N$ (period: 10 to 20 December 2013, dashed: descending node, solid: ascending node). Red lines show the tracks of conducted HALO research flights. The green line indicates the profile discussed in Section 3.1 Black dots mark locations of dropsondes.

Table 1. Overview of the conducted research flights during NARVAL (times given in UTC).

Date	Take-off	Underflight	Landing
10.12.2013	10:14 (EDMO)	15 : 08*	20:41 (TBPB)
11.12.2013	14:29 (TBPB)	17 : 26	21:58 (TBPB)
12.12.2013	13:50 (TBPB)	16 : 30	20:20 (TBPB)
14.12.2013	13:35 (TBPB)	16 : 18	20:21 (TBPB)
15.12.2013	15:15 (TBPB)	17 : 01	21:45 (TBPB)
16.12.2013	13:10 (TBPB)	16 : 07	22:59 (EDMO)
19.12.2013	10:05 (EDMO)	-	19:57 (TBPB)
20.12.2013	16:20 (TBPB)	17 : 19	02:35 (EDMO)

* excluded in analysis

2.2 Lidar systems

For this study we use measurements of airborne and spaceborne lidar instruments. Both are briefly described in the following.

2.2.1 The WALES instrument

The lidar system WALES (Water vapour Lidar Experiment in Space; Wirth et al. (2009)) is an airborne system designed and built at the Institute of Atmospheric Physics of the German Aerospace Centre (DLR). It measures the water vapor mixing ratio using differential absorption lidar technique at four wavelengths in the absorption bands of water vapor around 935 nm. Additionally, WALES is equipped with high spectral resolution lidar (HSRL) channel at 532 nm using an iodine filter (Esselborn et al., 2008). Furthermore, WALES performs polarization sensitive measurements at 532 and 1064 nm. WALES raw data have a vertical resolution of 15 m and a temporal resolution of 0.1 s. In this study we use the retrieved particle backscatter coefficient β_{part} at 532 nm with a vertical resolution of 15 m and a temporal resolution of 1 s resulting in a horizontal resolution of $\sim 200\ m$ at a typical aircraft speed of 200 ms^{-1}.

2.2.2 The CALIOP instrument

The CALIPSO satellite has a sun synchroneous orbit in an altitude of about 705 km with nadir-pointing orientation. It crosses the equator at 13:30 (ascending node) and 01:30 (descending node) local solar time and has a 16-day repeat cycle. CALIOP is the spaceborne lidar instrument (Winker et al., 2007) on-board CALIPSO (Winker et al., 2010). It is a backscatter lidar performing simultaneous polarization sensitive measurements at 532 and 1064 nm. CALIOP data are provided in different data processing levels. For this study we use the total attenuated backscatter coefficient β_{tot} of CALIOP Level 1B V4 532 nm data, which has a vertical resolution of 30 m and a horizontal resolution of 330 m.

2.3 Data evaluation

For a consistent comparison of the WALES and CALIOP instruments data sets need to be converted into a uniform unit. Therefore we use the backscatter ratio, given by the equation: $BSR = \beta_{tot}/\beta_{mol} = 1 + \beta_{part}/\beta_{mol}$. Hereby, β_{part} and β_{tot} are directly measured from the WALES and CALIOP instrument, respectively. As the scattering cross section of atmospheric gases is well known, the molecular backscatter coefficient β_{mol} can be easily calculated using temperature (T) and pressure (p) profiles. In this study we obtain temperature and pressure information from the Integrated Forecasting System model analysis (IFS) of the European Centre for Medium-range Weather Forecasts (ECMWF). The modelled fields are interpolated in space and time to match the flight paths of CALIPSO and HALO and the specific vertical resolutions of WALES and CALIOP.
To determine cloud top heights based on the BSR data, we define a BSR threshold for the cloud-/no-cloud decision. Threshold methods for cloud detections in lidar profiles are well known and provide a good basis for the estimation of cloud size parameters (e.g. Medeiros et al. (2010), Nuijens et al. (2009) or Nuijens et al. (2014)). In the period of NARVAL, typical aerosol BSR in the marine boundary layer ranged from 4 to 20, however, soaked aerosol layers can reach far larger BSR values. Clouds however, were observed to have BSR values > 80 during NARVAL. Thus we use the empirical value of $BSR = 90$

for the cloud/no-cloud decision. To avoid surface echoes we exclude the lowermost 250 m (all heights are given in heights above sea level) above the surface. The cloud detection algorithm scans profiles in the direction of beam propagation. If the threshold is exceeded once in a single lidar shot, the corresponding cloud top height is marked and the profile is flagged as cloudy (Figure 2).

In a next step, all cloudy profiles are connected to determine cloud size distributions along the flight-paths. At least one cloud-free profile is needed in-between to separate two cloudy sections into independent clouds. Otherwise, they are attributed to the same cloud. For the calculation of cloud length and cloud gap length we assume a spherical shape of the Earth and take the cloud top height of the considered cloud into account.

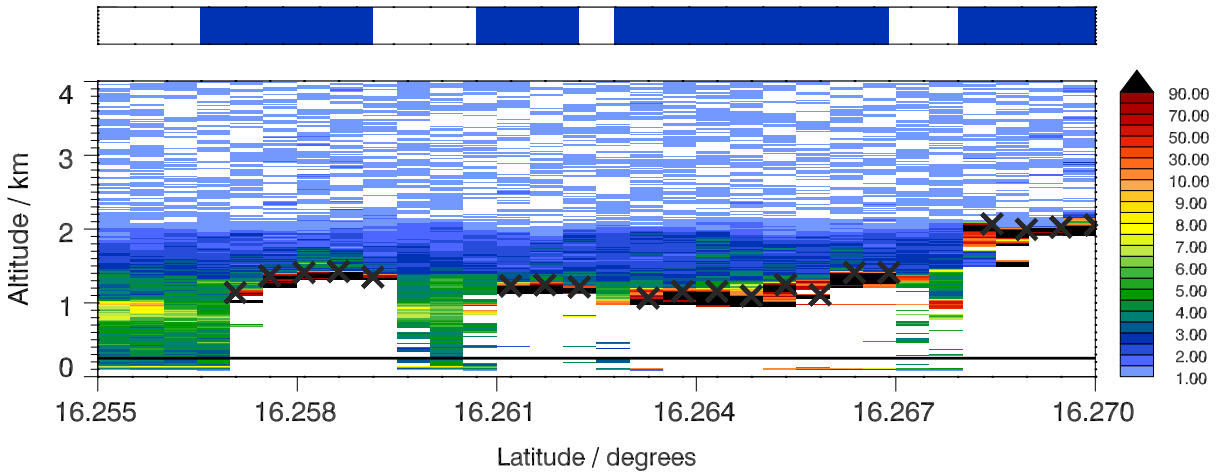

Figure 2. Exemplary visualisation of the developed algorithm applied on WALES data along the flight track. Colors represent measured backscatter ratios. Grey crosses indicate detected cloud tops. The horizontal solid black line marks the surface echo cut-off. The uppermost panel shows sequences of detected clouds (blue-filled polygons).

3 Results

Six A-Train underflights in the research area in the trades were performed during the NARVAL campaign. Collected data sets during these underflights enable direct comparisons of CALIOP and WALES measurements.

3.1 Case study - 11 December 2013

The synoptic situation over the Carribean Ocean on 11 December 2013 is characterized by small irregularly scattered clouds with embedded stratiform clouds over the Carribean Ocean. South of $\sim 12°$ N, deep convective structures related to the inter-tropical convergence zone (ITCZ) are present. On that day, airborne lidar measurements were conducted west of Barbados (between $10°$ N and $18°$ N - Figure 3 (left)).

During the research flight, a CALIPSO underflight was performed on a flight track reaching from $14.1°$ N, $57.2°$ W to $16.9°$ N, $57.8°$ W, also marked in Figures 1 and Figure 3. The colocated BSR cross-sections of WALES and CALIOP (~ 320 km) are shown in Figure 4. CALIPSO passed this flight track in less than one minute. HALO needed 35 minutes (17:13 - 17:37 UTC) to sample the profile.

A lower signal-to-noise-ratio of the CALIOP instrument compared to the WALES instrument is apparent at first glance. As a result, aerosol structures in CALIOP measurements can hardly be distinguished. Cloud structures however, are detected by both instruments. Differences in the two measured cross-sections are mainly seen at the beginning of the underflight. Due to the different speeds of HALO and CALIOP, especially highly variable cloud structures may have changed at the beginning and end of the track. Between latitudes of $15.1°$ N and $16.2°$ N, spanning over approximately 125 km, the situation is dominated by an elevated cloud structure. Besides this cloud structure small-scale convective clouds with horizontal extents of less than 1 km are present.

The cloud top height fraction along the flight paths is given by, $CTH_{fraction} = N_{CTH(\Delta z)}/N_{CTH(tot)}$, where $N_{CTH(\Delta z)}$ is the number of detected cloud top heights in each bin interval of the distribution and $N_{CTH(tot)}$ is the total number of detected cloud tops in the range from 0 to 4 kilometers altitude. Distributions of cloud top height fractions along the flight track are in good agreement, both showing a two-layer cloud structure. Both distributions have their maximum in detected frequency in

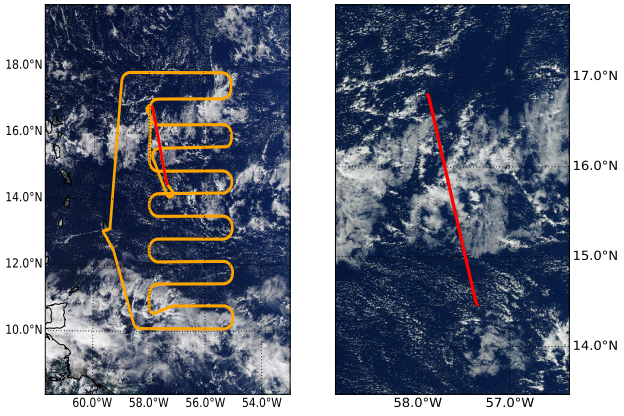

Figure 3. RGB satellite images taken from MODIS. The orange line illustrates the flight path of the HALO research aircraft during the research flight on 11 December 2012 (left). The red line indicates the flight track of the CALIPSO satellite underflight (right).

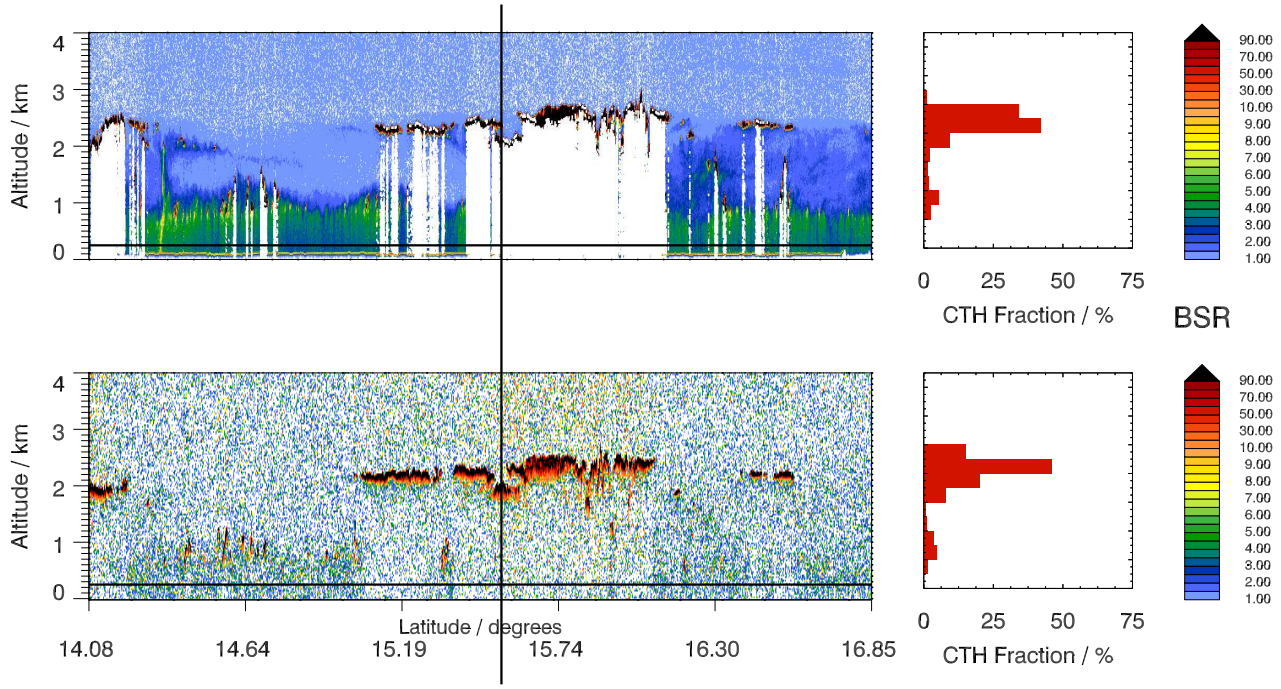

Figure 4. Vertical profiles of determined BSR during a CALIPSO underflight on 11 December 2013 (WALES (top) and CALIOP profiles (bottom)). The cloud top detection algorithm is applied above 250 m (horizontal black solid line). The CALIPSO overpass is marked by the black vertical line. Cloud top height fractions are shown in the right hand side histograms with 250 m vertical bin-size.

heights from 2250 to 2500 m due to the extensive cloud layer in the middle of the lidar cross section. Over 47% of all cloud top heights derived from CALIOP measurements and 43% derived from WALES measurements are found in this height range. However, while the distribution obtained from WALES measurements shows high values in the height bins 2250-2500 m and 2500-2750 m with 43% and 32%, respectively, the distribution derived from CALIOP measurements shows a contribution of almost 50% in the height bin between 2250-2500 m, but a significantly lower value above. In contrast it shows about 10% more cloud top heights located in heights between 2000 and 2250 m compared to the distribution derived from WALES measurements. Both distributions show local maxima in the order of 5% in height bins between 750 and 1250 m, representing the small-scale convective clouds. No cloud tops are detected above 3000 m.

3.2 Cloud top heights

In a next step we take a closer look on derived cloud top heights from CALIOP underflight measurements during NARVAL (Figure 5 (a)). An overview of the number of used data sets and profile kilometers is given in Table 2.

The distribution of all conducted underflights (Figure 5(a)) indicates, that more than 50% of the detected cloud tops derived

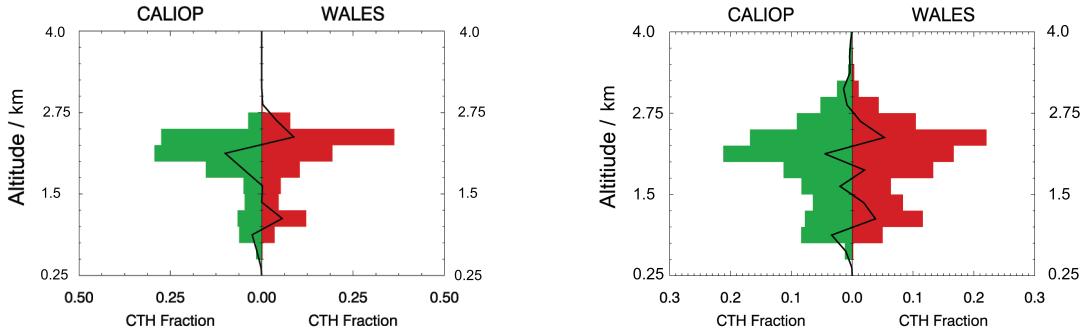

Figure 5. Relative frequency distributions of detected cloud top heights measured by WALES and CALIOP - (a) during all conducted CALIPSO underflights and (b) during the whole NARVAL period (spatial boundaries: 60 and 35° W and 10 and 20° N). The black lines indicate the differences between the compared profiles for each bin-interval with a bin-size of 250 m.

from measurements of both instruments are found in heights between 2000 to 2500 m. As already seen in the case study on 11 December 2013, the cloud top height distribution derived from WALES measurements shows larger values in the uppermost part of the height range from 2000 to 2500 m while the CALIOP derived distribution shows a higher contribution in the lower part. Furthermore, the distributions derived from both instruments have a local maximum in heights between 1000 and 1250 m, with WALES detecting an almost doubled percentage of cloud tops than CALIOP in this height region (WALES: $\sim 15\%$; CALIOP: $\sim 7\%$). Overall, differences in relative frequency in each bin interval between the two data sets never exceed 10%. There are no overall systematic differences in the distributions, although WALES data shows a more pronounced bimodal structure.

Table 2. Overview of the used data sets during the NARVAL period listing the profile kilometers in the area ranging from $60°W$ to $35°W$ and $10°$ to $20°N$ (period: 10 to 20 December 2013).

	Profile km
Underflights	$\sim 2300\ km$
WALES Data (NARVAL period)	$\sim 32000\ km$
CALIOP Data (NARVAL period)	$\sim 24500\ km$

Next, we go more into detail and compare measurements from both instruments along the flight path. In particular, we compare differences in detected cloud top heights along the underflight. Hereby, CALIOP profiles are matched to corresponding WALES profiles by nearest-neighbor interpolation. This interpolation enables a direct comparison of detected cloud top heights derived from both instruments along the underflight. Figure 6 (left) illustrates the distribution of cloud top height differences from all WALES and CALIPSO underflight measurements for profiles in which both instruments detected a cloud. A distinct maximum is seen in the interval ranging from 0 to 15 meters. On both sides of the maximum the frequency of cloud top height differences

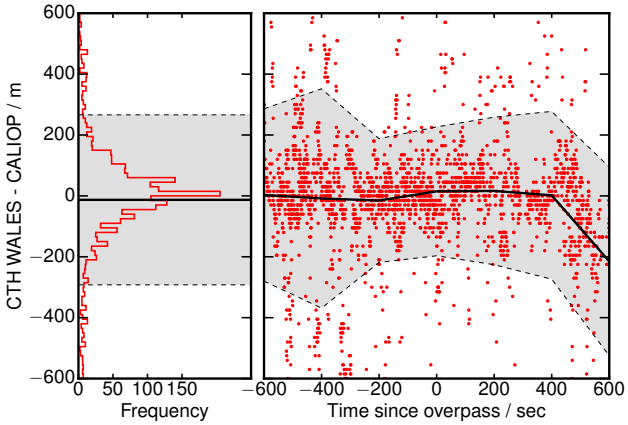

Figure 6. Distribution of differences in detected cloud top heights (CTH) between CALIOP and WALES (left) with bin intervals of 15 m. The gray shading marks the area of one standard deviation (1σ). Differences in detected cloud top heights between CALIOP and WALES as a function of temporal difference between both instruments (right).

decreases in a symmetric manner. As a result, the mean difference in detected cloud tops results in just -8 meters. The standard deviation adds up to 300 meters. The spread of detected cloud top heights can be explained by small horizontal offsets of WALES and CALIOP measurements along the flight track and the fact that CALIPSO is ~ 38 times faster (7500 ms^{-1} compared to ~ 200 ms^{-1}). Consequential, cloud structures may have changed in the period between WALES and CALIOP measurements. Moreover, the different lidar beam diameters and the inter-profile region not sampled by CALIOP are contributing factors.

Figure 6 (right) shows the difference in detected cloud top heights as a function of elapsed time since the CALIPSO overpass. The scatterplot indicates, that differences in detected cloud top heights of CALIOP and WALES are smallest, when the temporal separation between the two instruments is small. Peak values of the standard deviation are located at times of large temporal separation of the two instruments. The mean difference is always located around zero, except at times from 400 to 600 seconds. The sudden decrease at times from 400 to 600 seconds is related to the end of the underflights, when HALO was leaving the CALIOP track. However, cloud structures from -600 to +400 did not change significantly.

So far we have investigated differences in shallow marine cloud top height detection during all conducted underflights. Next we want to compare the cloud top height distribution derived from all CALIOP measurements with the one derived from all WALES measurements during the period of NARVAL (Figure 5(b)). The overall shape of the distributions is in good agreement. Again, a bimodal structure is obvious with maxima in heights from 750 to 1500 and 1750 to 2500 m. The maximum derived from WALES measurements is found between 2250 and 2500 m, while the maximum in CALIOP measurements is found in heights from 2000 to 2250 m. Altogether, about 60% of all cloud tops are located in the interval from 1750 to 2750 m for both lidar systems. In the height range between 750 and 1500 m, $\sim 21\%$ (CALIOP) and ~ 25 % (WALES) of all detected clouds were found.

The bimodal structure derived from both instruments agrees well with findings by Medeiros et al. (2010), who compare airborne backscatter lidar measurements during the Rain in Cumulus Over the Ocean campaign (RICO - Dec 2004 to Jan 2005, Rauber et al. (2007)) with CALIOP cloud measurments. They found maxima in heights from 0.75 to 1 km and 2.0 to 2.5 km. Moreover, the distribution found in this study is in agreement with cloud top heights derived from passive satellite measurements with 90 m spatial resolution (Genkova et al., 2007). A study, investigating the extents of optically thin and optically thick clouds, also found a bimodal structure in the vertical cloud top distribution and suggest, that the lower mode mainly consists of small cumuli and fragments of clouds with insufficient buoyancy for deepening (Leahy et al., 2012).

3.3 Cloud lengths and cloud gap lengths

Figure 7 shows the frequency distributions of detected cloud lengths by WALES and CALIOP during the whole period of NARVAL and in the predefined measurement area.

During NARVAL shallow marine clouds with horizontal extens of less than 1 km were prevalent. They make up 75% in WALES measurements and 60% in analyzed CALIOP data sets. 62% of all clouds in WALES measurements have horizontal extents of less than 0.5 km, whereas CALIOP only detects 46% in this interval. However, CALIOP detects 6% more clouds in

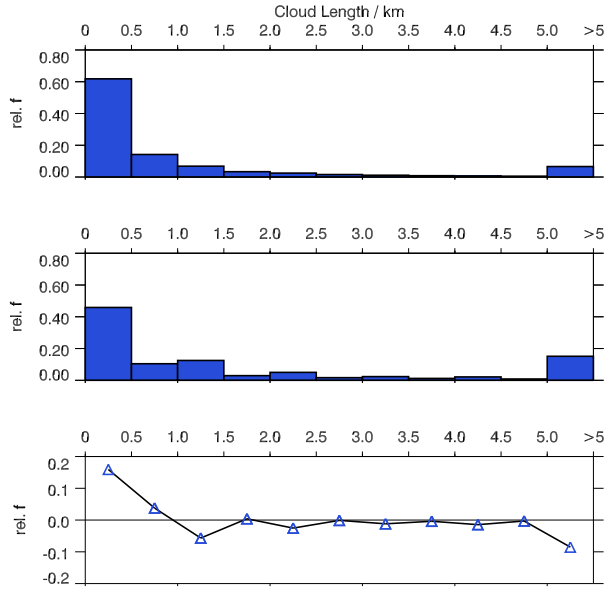

Figure 7. Relative distribution of cloud lengths of WALES (top) CALIOP measurements (middle) in the period from 10 to 20 December 2013 and in longitudes of 60° to 35° W and latitudes of 10° to 20° N. The lower panel shows the difference in detected cloud lenghts for each bin interval (rel.f.$_{WALES}$-rel.f.$_{CALIOP}$).

the size range from 1 to 2 km. The significant difference of 16% in cloud fraction of clouds < 0.5 km might be explained by the sparse sampling rate of the CALIOP instrument compared to the WALES instrument. CALIOP lidar beams have a diameter of 90 m on the ground, but the horizontal separation between two consecutive lidar shots is 330 m. As a result, areas between consecutive 'cloudy' lidar profiles, are assumend to be cloudy as well, leading to an underestimation of small cloud length amount and contributing to the amount of longer clouds. Thus, CALIOP measurements indicate 9% more clouds longer than 5 km, than WALES (WALES: 6%; CALIOP: 15%). The distribution of cloud lengths greater than 1.5 km do not show significant differences and indicate an exponential decrease in cloud lengths frequency with cloud length. The derived total cloud fraction during NARVAL adds up to 37% in both WALES and CALIOP data sets. Hereby, the cloud fraction is calculated according to $CF = \sum N_{cloudy} / \sum (N_{clear} + N_{cloudy})$, where N_{cloudy} is the number of vertical lidar profiles marked as cloudy and N_{clear} is the number of vertical lidar profiles marked as clear. The calculated cloud fraction is in agreement with groundbased measurements at the Barbados cloud observatory (Nuijens et al., 2014).

Figure 8 illustrates the length distribution of cloud-free areas from WALES and CALIOP data in the period of NARVAL. WALES profiles show an exponential decraese in cloud gap frequency with gap length. WALES measurements indicate 48 % of cloud lengths being smaller than half a kilometre. The distribution of CALIOP measurements however, suggests that only a portion of 29 % is smaller than 500 meters. The difference is again explained by the spare sampling rate of CALIOP. Cloud

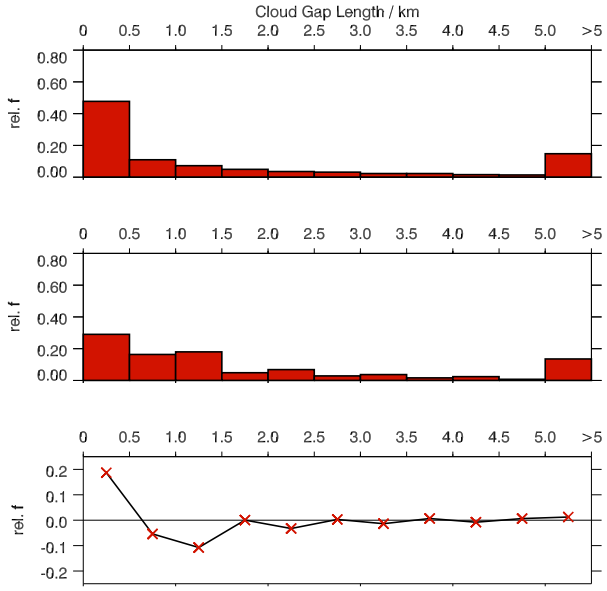

Figure 8. Relative distribution of cloud gap lengths of WALES (top) CALIOP measurements (middle) in the period from 10 to 20 December 2013 and in longitudes of 60° to 35° W and latitudes of 10° to 20° N. The lower panel shows the difference in detected gap lenghts for each bin interval (rel.f.$_{WALES}$-rel.f.$_{CALIOP}$).

gaps with extents twice or thrice the resolution are overestimated, since the area between two cloud-free profiles is assumed to be cloud-free as well. This is why CALIOP detects 5% more cloud gap lengths than WALES in the interval from 0.5 to 1.0 km length and 10% more in the interval from 1.0 to 1.5 km length in our measurements.

Detected WALES and CALIOP gap lengths longer than 5 km make up 14% and 15%, respectively. Varnai and Marshak (2011) found, that 50 % of all marine clouds over ice free oceans are separated less than 5 km from each other. Our observations indicate, that this fraction increases to $> 85\%$, when analyzing shallow cloud regimes in North Atlantic trade wind regions.

4 Conclusion

The observation of cloud-size parameters in trade wind regions is of high importance for the development, evaluation and validation of numerical models. Airborne instruments provide measurements with great temporal and spatial coverage and allow measurements of desired quantities form the top of the atmosphere down to the Earth's surface. Moreover, satellite-coordinated research flights enable comparisons of airborne with spaceborne measurements, allowing to validate satellite measurements.

In contrast, ground based lidar instruments allow measurements in the opposite direction from the ground to the top of the atmosphere, providing information on cloud base heights of shallow marine cumulus convection (e.g. Nuijens.2014). Ground based lidar and radar measurements, however, have one main limitation: no information on the horizontal extent of clouds can be retrieved without assumptions on wind speed and subsequent advection processes. This is why airborne field campaigns like NARVAL are from high importance.

During the NARVAL mission, advantages of advanced lidar measurements onboard a research aircraft, that enables measurements in high altitudes and over long distances, were exploited to study shallow marine cumulus convection. NARVAL also allowed to compare satellite based lidar measurements with airborne lidar measurements over large distances.

Statistics of shallow marine cloud top height distributions from WALES and CALIOP are in good agreement. However, cloudy/cloud-free segments of less than 330 m extent cannot be resolved by the CALIOP instrument. This results in an underestimation of small cloud and cloud gap lengths.

Acknowledgements. The authors like to thank the staff members of the DLR HALO aircraft from DLR Flight Experiments for preparing and performing the measurement flights. All CALIPSO data were obtained from NASA Langley Research Center Atmospheric Science Data Center. Profiles of atmospheric parameters, e.g. pressure and temperature, were provided by ECMWF. The data used in this publication was gathered in the NARVAL (Next-generation Aircraft Remote-Sensing for Validation Studies) campaign and is made available through the DLR Institute for Atmospheric Physics. NARVAL was funded with support of the Max Planck Society, the German Research Foundation (DFG), the European Research Council (ERC), the German Meteorological Weather Service (DWD) and the German Aerospace Center (DLR). This study was funded by a DLR VO-R young investigator group within the Institute of Atmospheric Physics.

References

Bony, S. and Dufresne, J.-L.: Marine boundary layer clouds at the heart of tropical cloud feedback uncertainties in climate models, Geophys. Res. Lett., 32, doi:10.1029/2005GL023851, 2005.

Colòn-Robles, M., Rauber, R. M., and Jensen, J. B.: Influence of low-level wind speed on droplet spectra near cloud base in trade wind cumulus, Geophys. Res. Lett., 33, doi:10.1029/2006GL027487, 2006.

Esselborn, M., Wirth, M., Fix, A., Tesche, M., and Ehret, G.: Airborne high spectral resolution lidar for measuring aerosol extinction and backscatter coefficients, Appl. Opt., 47, 346–358, doi:10.1364/AO.47.000346, 2008.

Genkova, I., Seiz, G., Zuidema, P., Zhao, G., and Girolamo, L. D.: Cloud top height comparisons from ASTER, MISR, and MODIS for trade wind cumuli, Remote. Sens. Environ., 107, 211–222, doi:10.1016/j.rse.2006.07.021, 2007.

Hartmann, D. L., Ockert-Bell, M. E., and Michelsen, M. L.: The effect of cloud type on Earth's energy balance: Global analysis, J. Clim., 5, 1281–1304, doi:10.1175/1520-0442(1992)005<1281:TEOCTO>2.0.CO;2, 1992.

Klepp, C., Ament, F., Bakan, S., Hirsch, L., and Stevens, B.: NARVAL campaign reoprt, Report, Max Planck Institiut für Meteorologie, 2014.

Krautstrunk, M. and Giez, A.: The transition from FALCON to HALO era airborne atmospheric research, in: Atmospheric Physics, edited by Schumann, U., Research Topics in Aerospace, pp. 609–624, Springer Berlin Heidelberg, 2012.

Leahy, L. V., Wood, R., Charlson, R. J., Hostetler, C. A., Rogers, R. R., Vaughan, M. A., and Winker, D. M.: On the nature and extent of optically thin marine low clouds, Geophys. Res. Lett., 117, doi:10.1029/2012JD017929, 2012.

Mech, M., Orlandi, E., Crewell, S., Ament, F., Hirsch, L., Hagen, M., Peters, G., and Stevens, B.: HAMP - the microwave package on the High Altitude and LOng range research aircraft HALO, Atmos. Meas. Tech., 7, 4539–4553, doi:10.5194/amtd-7-4623-2014, 2014.

Medeiros, B., Nuijens, L., Antoniazzi, C., and Stevens, B.: Low-latitude boundary layer clouds as seen by CALIPSO, J. Geophys. Res. Atmos., 115, doi:10.1029/2010JD014437, d23207, 2010.

Nuijens, L., Stevens, B., and Siebesma, A. P.: The Environment of Precipitating Shallow Cumulus Convection, J. Atmos. Sci., 66, 1962–1979, doi:10.1175/2008JAS2841.1, 2009.

Nuijens, L., Serikov, I., Hirsch, L., Lonitz, K., and Stevens, B.: The distribution and variability of low-level cloud in the North Atlantic trades, Q. J. Roy. Meteor. Soc., 140, 2364–2374, doi:10.1002/qj.2307, http://dx.doi.org/10.1002/qj.2307, 2014.

Rauber, R. M., III, H. T. O., Girolamo, L. D., Göke, S., Snodgrass, E., Stevens, B., Knight, C., Jensen, J. B., Lenschow, D. H., Rilling, R. A., Rogers, D. C., Stith, J. L., Albrecht, B. A., Zuidema, P., Blyth, A. M., Fairall, C. W., Brewer, W. A., Tucker, S., Lasher-Trapp, S. G., Mayol-Bracero, O. L., Vali, G., Geerts, B., Anderson, J. R., Baker, B. A., Lawson, R. P., Bandy, A. R., Thornton, D. C., Burnet, E., Brenguier, J.-L., Gomes, L., Brown, P. R. A., Chuang, P., Cotton, W. R., Gerber, H., Heikes, B. G., Hudson, J. G., Kollias, P., Krueger, S. K., Nuijens, L., O'Sullivan, D. W., Siebesma, A. P., and Twohy, C. H.: Rain in Shallow Cumulus Over the Ocean: The RICO Campaign, Bull. Am. Meteorol. Soc., 88, 1912–1928, doi:10.1175/BAMS-88-12-1912, 2007.

Siebert, H., Beals, M., Bethke, J., Bierwirth, E., Conrath, T., Dieckmann, K., Ditas, F., Ehrlich, A., Farrell, D., Hartmann, S., Izaguirre, M. A., Katzwinkel, J., Nuijens, L., Roberts, G., Schäfer, M., Shaw, R. A., Schmeissner, T., Serikov, I., Stevens, B., Stratmann, F., Wehner, B., Wendisch, M., Werner, F., and Wex, H.: The fine-scale structure of the trade wind cumuli over Barbados - An introduction to the CARRIBA project, Atmos. Chem. Phys., 13, 10 061–10 077, doi:10.5194/acp-13-10061-2013, 2013.

Stephens, G. L., Vane, D. G., Boain, R. J., Mace, G. G., Sassen, K., Wang, Z., Illingworth, A. J., O'Connor, E. J., Rossow, W. B., Durden, S. L., Miller, S. D., Austin, R. T., Benedetti, A., C, M., and the CloudSat Science Team.: The CloudSat Mission and the A-Train, B. Am. Meteorol.. Soc., 83, 1771–1790, doi:10.1175/BAMS-83-12-1771, 2002.

Stevens, B.: Atmospheric moist convection, Annu. Rev. Earth Planet. Sci., 33, 605–643, doi:10.1146/annurev.earth.33.092203.122658, 2005.

Varnai, T. and Marshak, A.: Global CALIPSO Observations of Aerosol Changes Near Clouds, IEEE Geosci. Remote. S., 8, 19–23, doi:10.1109/lgrs.2010.2049982, 2011.

Winker, D. M., Hunt, W. H., and McGill, M. J.: Initial performance assessment of CALIOP, Geophys. Res. Lett., 34, 8–15, doi:10.1029/2007GL030135, 2007.

Winker, D. M., Pelon, J., Coakley, J. A., Ackerman, S. A., Charlson, R. J., Colarco, P. R., Flamant, P., Fu, Q., Hoff, R. M., Kittaka, C., Kubar, T. L., Le Treut, H., McCormick, M. P., Mégie, G., Poole, L., Powell, K., Trepte, C., Vaughan, M. A., and Wielicki, B. A.: The CALIPSO mission: A global 3D view of aerosols and clouds, Bull. Am. Meteor. Soc., 91, 1211–1229, doi:10.1175/2010BAMS3009.1, 2010.

Wirth, M., Fix, A., Mahnke, P., Schwarzer, H., Schrandt, F., and Ehret, G.: The airborne multi-wavelength water vapor differential absorption lidar WALES: system design and performance, Appl. Phys. B, 96, 201–213, doi:10.1007/s00340-009-3365-7, 2009.

Wood, R. and Field, P.: Relationships between Total Water, Condensed Water, and Cloud Fraction in Stratiform Clouds Examined Using Aircraft Data, Journal of the Atmospheric Sciences, 57, 1888–1905, doi:10.1175/1520-0469(2000)057<1888:RBTWCW>2.0.CO;2, 2000.

Zelinka, M. D., Klein, S. A., and Hartmann, D. L.: Computing and partitioning cloud feedbacks using cloud property histograms. Part I: Cloud radiative kernels, J. Clim., 25, 3715–3735, doi:10.1175/JCLI-D-11-00248.1, 2012.